Article:
Korzeniewski, B and Rossiter, HB (2015) Each-step activation of oxidative phosphorylation is necessary to explain muscle metabolic kinetic responses to exercise and recovery in humans. Journal of Physiology, 593 (24). pp. 5255-5268. ISSN 0022-3751

https://doi.org/10.1113/JP271299

Each-step activation of oxidative phosphorylation is necessary to explain muscle metabolic kinetic responses to exercise and recovery in humans

Bernard Korzeniewski[1] and Harry B. Rossiter[2,3]

[1]*Faculty of Biochemistry, Biophysics and Biotechnology, Jagiellonian University, Kraków, Poland*

[2]*Rehabilitation Clinical Trials Center, Division of Respiratory & Critical Care Physiology & Medicine, Los Angeles Biomedical Research Institute at Harbor-UCLA Medical Center, Torrance, CA, USA.*

[3]*School of Biomedical Sciences, Faculty of Biological Sciences, University of Leeds, Leeds, UK.*

Running title: Each-step activation of OXPHOS in human muscle during exercise transitions

Keywords: human skeletal muscle; exercise; oxygen uptake

Correspondence: B. Korzeniewski, Faculty of Biochemistry, Biophysics and Biotechnology, Jagiellonian University, ul. Gronostajowa 7, 30-387 Kraków, Poland, tel. (48 12) 664 63 73, fax. (48 12) 664 69 02, e-mail: bernard.korzeniewski@gmail.com

Key points

- The basic control mechanisms of oxidative phosphorylation (OXPHOS) and glycolysis during work transitions in human skeletal muscle are still a matter of debate
- We used simulations of skeletal muscle bioenergetics to identify key system features that contribute to this debate, by comparing kinetic model outputs to experimental human data, including phosphocreatine (PCr), pH, pulmonary oxygen uptake and fluxes of ATP production by OXPHOS (vOX), anaerobic glycolysis and creatine kinase in moderate and severe intensity exercise transitions
- We found that each-step activation (ESA) of particular OXPHOS complexes, NADH supply and glycolysis, and strong (third-order) glycolytic inhibition by protons, was required to reproduce observed PCr, pH, and vOX kinetics during exercise
- A slow decay of ESA during recovery, which was slowed further following severe exercise, was necessary to reproduce experimental findings
- Well-tested computer models offer new insight in the control of the human skeletal muscle bioenergetic system during physical exercise

ABSTRACT

To better understand muscle bioenergetic regulation, a previously-developed model of the skeletal muscle cell bioenergetic system was used to simulate the influence of: 1) each step activation (ESA) of NADH supply (including glycolysis) and oxidative phosphorylation (OXPHOS) complexes; and 2) glycolytic inhibition by protons, on the kinetics of ATP synthesis from OXPHOS, anaerobic glycolysis and creatine kinase (CK). Simulations were fitted to previously published experimental data of ATP production fluxes and metabolite concentrations during moderate and severe intensity exercise transitions in bilateral knee-extension in humans. Overall, computer simulations agreed well with experimental results. Specifically, a large (>5-fold) direct activation of all OXPHOS complexes was required to simulate measured phosphocreatine (PCr) and OXPHOS responses to both moderate and severe intensity exercise. In addition, slow decay of ESA was required to fit PCr recovery kinetics, and the time constant of ESA decay was slower following severe (180s) than moderate (90s) exercise. Additionally, a strong inhibition of (anaerobic) glycolysis by protons (glycolytic rate inversely proportional to the cube of proton concentration) provided the best fit to the experimental pH kinetics, and may contribute to the progressive increase in oxidative ATP supply during acidifying contractions. During severe-intensity exercise an 'additional' ATP usage (a 27% increase at 8 min, above the initial ATP supply) was necessary to explain the observed $\dot{V}O_2$ slow component. Thus parallel activation of ATP usage and ATP supply (ESA), and a strong inhibition of ATP supply by anaerobic glycolysis, were necessary to simulate the kinetics of muscle bioenergetics observed in humans.

Abbreviations

A_{GL}, relative activation of glycolysis; A_{OX}, relative activation of oxidative phosphorylation; A_{UT}, relative activation of ATP utilization; AK, adenylate kinase; CK, creatine kinase; ESA, each-step activation; KE, bilateral knee extension exercise; MAS, malate/aspartate shuttle; Moderate glycolysis inhibition by H^+, first-order dependence on H^+; NADH, nicotinamide adenine dinucleotide; OXPHOS, oxidative phosphorylation; PCr, phosphocreatine; P_i, inorganic phosphate; Strong glycolysis inhibition by H^+, third-order dependence on H^+; S_{CK}, stoichiometry of proton production/consumption by CK; TCA, tricarboxylic acid cycle; vCK, muscle ATP production by creatine kinase; vGL, muscle ATP production by anaerobic glycolysis; vOX, muscle ATP production by oxidative phosphorylation; vUT, muscle ATP utilization (ATP hydrolysis); $\dot{V}O_2$, oxygen uptake (muscle or pulmonary).

INTRODUCTION

The basic mechanisms of the control of the skeletal muscle cell bioenergetic system, especially oxidative phosphorylation (OXPHOS), during work transitions is still a matter of debate. According to the original proposition by Chance and Williams (Chance & Williams, 1955), based on studies on isolated mitochondria, only ATP usage (actomyosin-ATPase and Ca^{2+}-ATPase) is directly activated by Ca^{2+} during rest-work transition in skeletal muscle, while the ATP-supply system, including O_2-consuming OXPHOS ($\dot{V}O_2$), is activated indirectly through negative feedback via increased sarcoplasmic concentration of the products of ATP hydrolysis: ADP and P_i. Several theoretical models assume, explicitly or implicitly, this mechanism (see e.g., Wilson et al., 1979; Wilson, 2015; Wu et al., 2007).

Jeneson and co-workers postulated that the mechanistic $\dot{V}O_2$-[ADP] dependence is at least second-order (Jeneson et al. 1996). The discovery that three TCA (tricarboxylic acid) cycle dehydrogenases (pyruvate dehydrogenase, isocitrate dehydrogenase, 2-oxoglutarate dehydrogenase) are activated by Ca^{2+} ions (Denton & McCormack, 1990; Hansford, 1980) led to the postulate that the NADH-supply system is directly activated together with ATP usage. This possibility was supported by the discovery of a large stimulation of $\dot{V}O_2$ in isolated brain mitochondria by Ca^{2+} ions acting through activation of the malate/aspartate shuttle (MAS) (Gellerich et al. 2012).

A general model of parallel activation of ATP usage and ATP supply during muscle contractions was postulated by Hochachka (1994), but this did not specify which particular enzymes/metabolic blocks in the ATP supply system were activated. It was subsequently proposed that not only ATP usage and NADH supply (including glycolysis), but also all OXPHOS complexes (complex I, complex III, complex IV, ATP synthase, ATP/ADP carrier, P_i carrier) are directly activated by some cytosolic mechanism predominantly involving cytosolic Ca^{2+} ions, calmodulin-like protein, and protein phosphorylation, during the rest-to-work transition in skeletal and heart muscle cells (Korzeniewski, 1998; Korzeniewski, 2003; Korzeniewski, 2007; Korzeniewski, 2014, Korzeniewski, 2015). This process is termed each-step-activation (ESA) (Korzeniewski, 2014). In skeletal muscle it is likely that a mixed

98 mechanism (MM) is manifest, in which all OXPHOS complexes are directly activated, but to a
99 smaller extent than ATP usage, and therefore a moderate increase in [ADP] and [P_i]
100 cooperates with ESA to bring about OXPHOS activation (Korzeniewski, 2014). In intact heart
101 muscle *in vivo* there is no (or extremely small) change in metabolite concentrations during
102 work transitions (Katz et al. 1989). Therefore, while high expression of OXPHOS
103 components may explain, in part, the a high sensitivity of ATP supply to very small changes
104 in muscle metabolites, a 'perfect' ESA, directly activating both ATP usage and OXPHOS to
105 the same extent, has been suggested to operate in intact heart *in vivo* (Korzeniewski, 2014).
106 The possibility of the parallel activation of ATP demand and ATP supply during rest-work
107 transition in skeletal muscle was supported by Wüst and co-workers (Wüst et al. 2011) on
108 the basis of experimental measurement of changes of muscle $\dot{V}O_2$ and [PCr] after the onset
109 of electrically-stimulated contractions in the canine hind limb. Nevertheless, evidence
110 supporting or refuting ESA has proven technically challenging in human muscle due to the
111 complexity involved in determining, at the necessary high temporal resolution, instantaneous
112 intramuscular metabolite concentrations, fluxes and relative activities of the various
113 components of the bioenergetics systems during exercise.
114 Additionally, it has been demonstrated both *in vitro* (see Connet & Sahlin, 1996 for
115 review) and in intact human skeletal muscle (Sutton et al. 1981) that cytosolic acidification
116 inhibits (anaerobic) glycolysis. Thus, during high-intensity exercise characterised by a
117 progressive metabolic acidosis, glycolytic inhibition may contribute to increasing the
118 demands of ATP provision from OXPHOS.
119 The ESA mechanism was proposed mainly on the basis of theoretical studies carried
120 out using a computer model of the skeletal muscle bioenergetic system developed previously
121 (Korzeniewski, 1998; Korzeniewski & Zoladz, 2001, Korzeniewski & Liguzinski, 2004). This
122 model includes a simple, semi-quantitative inhibition of glycolysis by protons, in which the
123 rate of glycolysis is inversely proportional to the instantaneous H^+ concentration (the simplest
124 possible description) (Korzeniewski & Liguziński, 2004). Recent investigation led to the
125 proposal that the inhibition of ATP supply from anaerobic glycolysis by progressive H^+ ion

accumulation, together with a slow decrease of ATP supply by creatine kinase (CK) and an additional progressive increase in ATP demand, may contribute importantly to the progressive increase in $\dot{V}O_2$ seen during high-intensity constant power exercise: the muscle $\dot{V}O_2$ slow component (Korzeniewski & Zoladz, 2015). The pulmonary $\dot{V}O_2$ slow component is generated principally within the exercising skeletal muscles (Poole et al., 1991).

While this computational model was extensively verified by comparison with various experimentally measured parameter and variable values and system properties (see e.g., Korzeniewski, 2007; Korzeniewski, 2014 for discussion), rarely has a direct comparison with biological data been made that would provide a satisfying, strictly quantitative, verification of the model and its postulates. This is mainly because the necessary *in vivo* measurements of several different variables during rest-work and work-rest transitions below the lactate threshold (moderate intensity) and above critical power (severe intensity), were not previously available. Recently, several different system variables, including time courses of pulmonary $\dot{V}O_2$, PCr and pH during transitions to and from moderate and severe intensity exercise as well as the rate of ATP supply by OXPHOS (vOX), CK (vCK) and anaerobic glycolysis (vGL) after 3 and 8 min of exercise during bilateral knee extension (KE) in humans were measured (Cannon et al. 2014). These data constitute an excellent reference point for computer model validation.

In this study, therefore, we tested the previously-developed computer model of the skeletal muscle bioenergetic system (Korzeniewski, 1998; Korzeniewski & Zoladz, 2001; Korzeniewski & Liguzinski, 2004) by direct comparison of computer simulations with published experimental data for transitions to and from moderate and severe intensity KE exercise in humans (Cannon et al. 2014). We hypothesized that a high intensity of ESA is necessary to account for the measured changes in fluxes and metabolite concentrations, as well as for the shape of time courses of these variables during transitions from rest to moderate or severe exercise and back to rest. We expected that ESA decays slowly during muscle recovery after exercise and that the characteristic decay time is longer after severe exercise than after moderate exercise. Finally, we tested the hypothesis that a progressive

154 increase in ATP usage during exercise and a strong glycolytic inhibition by protons in severe
155 intensity exercise could account for the relative magnitude of the $\dot{V}O_2$ and vOX slow
156 component measured *in vivo*.

METHODS

Ethical approval

The human data used in the present study for comparison with computational simulations were previously published (Cannon et al. 2014). All procedures were approved by The Biological Sciences Faculty Research Ethics Committee, University of Leeds, and the University of Liverpool Committee on Research Ethics, and complied with the latest revision of the Declaration of Helsinki. Written informed consent was obtained from all volunteers prior to their participation in the study. Further details on the experimental human data can be found in Cannon et al. (2014).

Computer model

The theoretical model of the skeletal muscle cell bioenergetics including anaerobic glycolysis developed by Korzeniewski and Liguzinski (2004), based on earlier models by Korzeniewski and Zoladz (2001) and Korzeniewski (1998), was used in the present study. This model comprises particular OXPHOS complexes (complex I, complex III, complex IV, ATP synthase, ATP/ADP carrier, P_i carrier), anaerobic glycolysis, CK, ATP usage, NADH supply, and proton efflux and influx.

The model has been broadly validated by comparison of its predictions with experimental data and used for numerous theoretical studies (see e.g., Korzeniewski, 2007; Korzeniewski, 2011, Korzeniewski 2014 for overview). The complete model description of the skeletal muscle bioenergetic system including anaerobic glycolysis is located on the web site: http://awe.mol.uj.edu.pl/~benio/.

Simulation procedures

We aimed to model the on- (rest-to-work) and off- (work-to-rest) transition during exercise in human skeletal muscle during bilateral KE (Cannon et al. 2014). These published data used magnetic resonance spectroscopy of the quadriceps and pulmonary $\dot{V}O_2$ to

measure the kinetics of muscle and whole-body bioenergetics during and following 3 and 8 min of moderate and severe intensity KE exercise in healthy young humans (n=13, one female; age, 27±8 years (mean ± SD); height, 177±8 cm; mass, 75±12 kg).

Simulations were made for two exercise intensities: moderate-intensity exercise below the lactate threshold and severe-intensity exercise above critical power. It should be noted that critical power was not measured in the original study of Cannon et al. (2014). However, based on the non-steady-state behaviour of pulmonary $\dot{V}O_2$ and intramuscular metabolism, the exercise intensity in Cannon et al. (2014) is here assumed to be above critical power (Poole et al. 1988; Jones et al. 2008): variably termed very-heavy or severe intensity exercise (see Rossiter, 2011 for discussion). Based on the experimental data we adjusted the activity (rate constant) of ATP usage (hydrolysis, A_{UT}) to be elevated 22 fold during transition from rest to moderate-intensity exercise, and 47 fold during transition from rest to severe-intensity exercise. This gave the value of muscle $\dot{V}O_2$ equal to about 2.6 mM/min (58 ml/kg/min) after 8 min of moderate-intensity exercise and to about 6.7 mM/min (150 ml/kg/min) after 8 min of severe-intensity exercise. Following this, model parameter values were adjusted independently for moderate and severe exercise, in order to best fit the experimental data for the kinetics of muscle PCr, pH, vOX, vCK, and vGL.

The activation of oxidative phosphorylation (A_{OX}; the relative increase of rate constants of complex I, complex III, complex IV, ATP synthase, ATP/ADP carrier, P_i carrier and NADH supply) (Korzeniewski, 1998; Korzeniewski, 2003; Korzeniewski, 2007; Korzeniewski, 2014) was adjusted following an exponential time course at exercise onset:

$$m_{OX} = A_{OX} - \left(A_{OX} - 1\right) \cdot e^{-t/\tau(ON_{OX})} \quad (1)$$

where m_{OX} is the current activation (ratio of the current rate constant to the resting rate constant) of OXPHOS, A_{OX} is the relative activation of OXPHOS during moderate and severe-intensity exercise, $\tau(ON_{OX})$ = 3 s is the characteristic time of the activation of oxidative phosphorylation (Korzeniewski, 2003) and t stands for the time after the onset of exercise. $\tau(ON_{OX})$ was small enough in order not to disturb the on-transient.

It was assumed that glycolysis was directly activated (A_{GL}) during rest to moderate and severe intensity exercise transitions, and the magnitude of A_{GL} was adjusted to best fit the experimental data. The need for this strong direct parallel activation of glycolysis was demonstrated previously (Korzeniewski & Liguzinski, 2004). The increase in the rate constant of glycolysis was not instantaneous, but occurred exponentially:

$$m_{GL} = A_{GL} - \left(A_{GL} - 1\right) \cdot e^{-t/\tau(ON_{GL})} \quad (2)$$

where m_{GL} is the current activation (ratio of the current rate constant to the resting rate constant of glycolysis), A_{GL} is the relative activation of glycolysis during exercise, $\tau(ON_{GL})$ = 6 s is the characteristic time for the activation of glycolysis and t stands for the time after the onset of exercise. $\tau(ON_{GL})$ was small enough in order not to disturb the on-transient.

After termination of exercise the rate constants of ATP usage and glycolysis were decreased instantly to the initial (rest) values. The rate constants of oxidative phosphorylation complexes decreased exponentially according to the following equation (Korzeniewski, 2003):

$$m_{OX} = 1 + \left(A_{OX} - 1\right) \cdot e^{-t/\tau(OFF_{OX})} \quad (3)$$

where m_{OX} is the current activation (ratio of the current rate constant to the resting rate constant) of OXPHOS, A_{OX} is the relative direct activation of OXPHOS during exercise, $\tau(OFF_{OX})$ = 90 s or 180 s is the characteristic decay time of the activation of oxidative phosphorylation for moderate and severe exercise, respectively, and t stands for the time after the onset of exercise.

There was no additional progressive component for ATP usage during moderate exercise. During severe exercise, in order to fit experimental data, a linear increase in ATP usage was included, beginning at 100 % of the 'fundamental' ATP usage rate (the rate at the immediate onset of exercise) and continuing until the end of exercise at 8 min (Paterson & Whipp, 1991; Barstow & Mole, 1991). This mechanism underlying the system behaviour of A_{UT} should not be confused with the behaviour of vOX itself (which is commonly approximated by a bi-exponential).

The influence of glycolytic inhibition by protons was interrogated using two different inhibitory states: moderate and strong. The rate of glycolysis for moderate glycolytic inhibition by protons was described by the following simple, semi-quantitative equation (as in Korzeniewski & Liguzinski, 2004):

$$v_{GLYC} = k_{GLYC} \cdot ADP_{te} \cdot \left(H^{+}_{rest} / H^{+}\right) \quad (4)$$

where k_{GLYC} is the rate constant of glycolysis, ADP_{te} is the cytosolic total (magnesium-bound and magnesium free) free ADP concentration, $H^{+}_{rest} = 10^{-7}$ M (pH = 7.0) is the resting proton concentration and H^{+} is the current proton concentration.

The rate of glycolysis for strong glycolytic inhibition by protons was described by the following simple equation:

$$v_{GLYC} = k_{GLYC} \cdot ADP_{te} \cdot \left(H^{+}_{rest} / H^{+}\right)^{3} \quad (5)$$

Therefore, it was assumed that the rate of glycolysis was inversely proportional to the cube of the current proton concentration.

Three computer simulations were carried out to identify the best-fit parameter values and conditions (A_{OX}, A_{GL}, $\tau(OFF_{OX})$, magnitude of 'additional' ATP usage, and moderate or strong inhibition of glycolysis by protons) during moderate and severe intensity exercise.

Simulation 1: Severe exercise with moderate glycolytic inhibition by protons.

Simulation 2: Severe exercise with strong glycolytic inhibition by protons.

Simulation 3: Moderate exercise with strong glycolytic inhibition by protons.

Simulations 1 and 2 first established the set of system characteristics that best fit the experimental data under conditions where fluxes, metabolite concentrations and, in particular, pH were most disturbed (severe exercise). Following this, simulation 3 was conducted using moderate exercise with the parameters of glycolytic inhibition established by the best fit from simulations 1 and 2.

263 **RESULTS**

264 The computer simulations performed in this study were compared with experimental
265 data for transitions to and from moderate and severe intensity KE exercise in humans
266 published previously (Cannon et al. 2014).

267 Figure 1 shows the results of Simulation 1. The best-fit model values with moderate
268 glycolytic inhibition by protons (Equ. 4), were A_{UT} = 47, A_{OX} = $47^{0.43}$ (5.24 fold), A_{GL} = $47^{0.65}$
269 (12.21 fold), $\tau(OFF_{OX})$ = 180 s, 'additional' ATP usage = 27 %. The simulated kinetics of PCr
270 (% of resting value) and pH, as well as the values of ATP supply by OXPHOS (vOX), CK
271 (vCK) and anaerobic glycolysis (vGL) at 3rd and 8th min of severe exercise with moderate
272 glycolytic inhibition by protons (Equ. 4) agreed well with the experimental data. Muscle $\dot{V}O_2$,
273 PCr, pH, ADP, vOX, vCK, vGL and ATP usage (vUT) did not reach a steady state, but
274 progressively changed during exercise ($\dot{V}O_2$, ADP, vUT and vOX increased, while PCr, pH,
275 vCK and vGL decreased). The main small differences between the simulation and the
276 experimental data were a slower decrease in pH and a smaller magnitude of the initial
277 transient alkalosis in the simulation. The former is most probably the result of insufficient
278 glycolytic inhibition by protons (see Simulation 2 below). The latter is likely due to the
279 stoichiometry of proton consumption and production by the CK in the Lohmann reaction. The
280 dependence of this stoichiometry on pH was extracted from the work of Kushmerick (1997)
281 and is S_{CK}=0.63-(pH-6.0)*0.43; which gives about 0.2 for pH ~7.0. For a higher value of S_{CK},
282 a more pronounced initial transient alkalosis was obtained in computer simulations (not
283 shown).

284 Additionally, a large slow component of the muscle $\dot{V}O_2$ on kinetics appeared in this
285 simulation (Simulation 1). It was caused mostly by the increase in ATP utilization during
286 exercise (from 100 to 127 % of the 'fundamental' rate of ATP turnover), but also, to a small
287 extent, by a moderate inhibition of ATP supply by anaerobic glycolysis (vGL) by
288 accumulating protons as exercise progressed, necessitating a supplementary increase in the
289 ATP supply from OXPHOS (vOX) (Korzeniewski & Zoladz, 2015).

The introduction of a strong glycolytic inhibition by protons (Equ. 5, glycolytic flux inversely proportional to the cube of the current proton concentration) for severe exercise, together with a stronger direct glycolytic activation at the onset of exercise (Simulation 2), significantly speeded the kinetics of the early intracellular pH response, but did not affect the pH value after 8 min of exercise. This can be seen in Fig. 2. In Simulation 2, with strong glycolytic inhibition by protons (Equ. 5), the model values were A_{UT} = 47, $A_{OX} = 47^{0.43}$ (5.24 fold), $A_{GL} = 47^{0.87}$ (28.49 fold), $\tau(OFF_{OX})$ = 180 s, 'additional' ATP usage = 27 %. This simulation gave a much better fit to the experimentally-measured time course of pH without influencing significantly the time course of PCr relative to the good fit observed in Simulation 1 (see Fig. 2). The high direct activation of (anaerobic) glycolysis led to a rapid decrease in pH after the onset of exercise, while the strong (anaerobic) glycolytic inhibition by protons that took place afterwards (slowing vGL) prevented excessive cytosolic acidification. Generally, an excellent agreement of theoretical predictions with experimental data was observed in this simulation. Not only time courses of PCr and pH, but also the values of ATP production by OXPHOS (vOX), CK (vCK) and anaerobic glycolysis (vGL) agreed well with the experimental data. The relative increase of the slow component of the muscle $\dot{V}O_2$ on-kinetics measured between 3 and 8 minutes of exercise in this simulation (20%) was similar to that of the measured pulmonary $\dot{V}O_2$ (22 ± 8%; Cannon et al. 2014). Anaerobic glycolysis was strongly directly activated after the onset of exercise, which significantly elevated the initial ATP synthesis by this process. However, as exercise progressed, glycolysis was strongly (third-order dependence) inhibited by accumulating protons, meaning that a significant additional fraction of ATP supply was provided by oxidative phosphorylation. The additional requirement for vOX can be observed in the reduction of vGL in Fig. 2, between the peak at ~0.75 min and end-exercise (8 min). In Simulation 2 both the strong (anaerobic) glycolytic inhibition by protons and the 'additional' ATP usage increasing during exercise from 0 % of the 'fundamental' ATP usage at the onset of exercise to 27 % after 8 min of exercise contributed to the slow component of the muscle $\dot{V}O_2$ on-kinetics.

317 Simulation 3 (for moderate exercise and strong glycolysis inhibition by protons) also
318 generally agreed very well with experimental data obtained by Cannon et al. (2014). This is
319 shown in Fig. 3. The model values for moderate exercise with strong glycolytic inhibition by
320 protons (Equ. 5) were $A_{UT} = 22$, $A_{OX} = 22^{0.56}$ (5.64 fold), $A_{GL} = 22^{0.85}$ (13.84 fold), $\tau(OFF_{OX})$ =
321 90 s, 'additional' ATP usage = 0 %. As expected, both experimental and simulated fluxes and
322 metabolite concentrations during moderate exercise rest-to-work and work-to-rest transitions
323 changed much less than during severe exercise. Additionally, unlike during severe exercise,
324 a steady-state was achieved after ~3 minutes of exercise. The only exception seems to be
325 the mean experimental measurement of vOX after 3 min of exercise is greater than the
326 simulation. vOX is 35 % greater at 3 min than after 8 min of moderate exercise. However,
327 while this difference is apparently big, as shown in the original presentation (Cannon et al.
328 2014) it was not statistically significant (see error bars in Fig. 3). Of course, a difference in
329 vOX between 3rd and 8th min of exercise could not be reconciled with the presence of the
330 steady-state in the time course of the pulmonary $\dot{V}O_2$, PCr and pH observed in this
331 experiment for moderate exercise (Cannon et al. 2014), and is likely the result of variability in
332 the measurement of this variable within subjects. However, it is not possible to know whether
333 the variability influences more the 3 min or 8 min values. Here, as in Cannon et al. (2014),
334 we assumed that the 3 min pulmonary $\dot{V}O_2$ value 'overshoots' the expected steady state,
335 albeit, non-significantly. Nevertheless, adjusting the simulations to give vUT (and vOX) that
336 was intermediate between the 3rd and 8th min of moderate exercise, namely 20 mM min^{-1}, did
337 not substantially change the relative agreement between the experimental and simulated
338 fluxes and metabolite concentrations (simulation not shown).

DISCUSSION

The first objective of this theoretical study was to determine whether a computer model of the skeletal muscle bioenergetic system (Korzeniewski, 1998; Korzeniewski & Zoladz, 2001; Korzeniewski & Liguzinski, 2004), was able to reproduce, strictly quantitatively, a particular concrete set of experimental data. Using the data from the experiment conducted by Cannon et al. (2014) as the frame of reference (because it involved simultaneous measurements of the time courses of PCr and pH for rest-work-rest transitions during moderate and severe exercise as well as vOX, vCK and vGL after 3 and 8 min of exercise), we found that overall the computer simulations produced a very good agreement with the experimental data (Figs. 1-3). This proved that the model was able to reproduce correctly the complex set of the modelled system properties, and allowed us to test 4 specific hypotheses of the relative intensity of ESA and glycolytic inhibition by protons in contributing to the observed metabolite concentrations and fluxes during moderate and severe intensity exercise.

Specifically, the important new findings of this study were that: 1. high-intensity ESA accounted for the system behaviour (changes in fluxes and metabolite concentrations during rest-work-recovery transitions) in human skeletal muscle during severe and moderate exercise (Figs. 2 and 3, respectively); 2. the decay of ESA after exercise was slow, and slowed further by severe-intensity, compared to moderate-intensity, exercise (Figs. 2 and 3); 3. strong (third-order dependence) glycolytic inhibition by protons better simulated the time course of pH during severe exercise (Fig. 2) than moderate glycolytic inhibition (Fig. 1); 4. the relative magnitude of the $\dot{V}O_2$ slow component *in vivo* was better modelled using a large additional ATP usage increasing progressively during exercise together with a strong proton inhibition of (anaerobic) glycolytic flux.

Each step activation (ESA) is obligatory for intramuscular bioenergetic flux control during exercise and recovery

This study emphasizes that an intensive ESA during exercise and slow decay of ESA after termination of exercise are obligatory to reproduce quantitatively the muscle metabolite concentrations and fluxes of experimental data. The direct activation of all OXPHOS complexes and NADH supply (A_{OX} in computer simulations) is over 5-fold, namely 5.64-fold and 5.24-fold during transition from rest to moderate and severe work, respectively. The A_{OX} is even slightly greater for moderate work, although the muscle $\dot{V}O_2$ is much greater for severe work, because the stability of PCr and pH is much better in the former case. $\dot{V}O_2$ is determined mostly by the ATP utilization rate (A_{UT}; as long as the OXPHOS capacity for ATP synthesis is not saturated in the absence of ESA, see below), while ESA intensity affects predominantly the stability of metabolite concentrations and their kinetics (Korzeniewski & Zoladz, 2004). The high predicted ESA intensity is not surprising, because the muscle $\dot{V}O_2$ increases 9.04 fold during the moderate rest-exercise transition, and 23.45 fold during the severe rest-exercise transition, while [ADP] increases only 2.17 fold and 5.49 fold, respectively. Therefore the phenomenological $\dot{V}O_2$-[ADP] relationship is very steep, much steeper than possible from first- or even second-order rate reactions. Even a steeper phenomenological $\dot{V}O_2$-[ADP] relationship is observed in some experiments (Wüst et al. 2011; Korzeniewski, 2014). For instance, it was observed that a 40-fold increase in electrically-stimulated dog muscle $\dot{V}O_2$ is accompanied by only 2.5-fold increase in [ADP] (Zoladz et al. 2008).

The fact that A_{OX} was smaller than A_{UT} implies that OXPHOS is directly activated in parallel with ATP usage during rest-to-work transition, but that OXPHOS activation is less than that of ATP usage. This corresponds to the mixed mechanism (MM) of bioenergetics control, where direct activation co-operates with negative-feedback activation (through an increase in [ADP] and [P_i]) in the control of OXPHOS (Korzeniewski, 2014) (see below).

Without ESA (A_{OX} = 1) the system collapses during severe exercise (A_{UT} = 47): [PCr] and [ATP] fall to zero (the latter is converted to ADP, and further, by adenylate kinase, AK, to AMP), [P_i] and [Cr] increase to maximal values, and a huge cytosolic acidification occurs while maximal muscle $\dot{V}O_2$ becomes limited to about 3.5 mM min^{-1}. Of course, this is only a

virtual prediction: in reality, in the absence of ESA, exercise would be slowed or terminated shortly after onset. Without ESA (A_{OX} = 1) during moderate exercise (A_{UT} = 22) and for lower ESA (say, for A_{OX} = 3) during moderate (A_{UT} = 22) and severe (A_{UT} = 47) exercise, the changes in metabolite concentrations predicted by the model are much greater than for high ESA, and therefore do not well fit the experimental data. Additionally, characteristic transition times (τ) for $\dot{V}O_2$ and metabolite concentrations during rest-work transitions are lengthened under conditions where lower ESA activities are used (Korzeniewski & Zoladz, 2004). Therefore, a decrease in ESA intensity in computer simulations results in wide disagreements with experimental results.

It was demonstrated previously, in the bioenergetic system of the skeletal muscle cell that, without ESA, huge changes in metabolite (ADP, PCr, P_i) concentrations take place when the relative ATP demand increases, and that the system collapses when the energy demand (rate constant of ATP usage) exceeds the relative value of about A_{UT} = 30 fold above resting ATP demand. Under these conditions ATP and PCr concentrations fall to zero, Cr and P_i concentrations rise to the maximal values, [ADP] first rises to about 1500 μM and then decreases near zero as it is converted to AMP (by AK) and there is no further increase in muscle $\dot{V}O_2$ together with an increase of ATP demand (see Fig. 3A in Liguzinski & Korzeniewski, 2006). In the present study, the relative ATP demand (A_{UT}) for severe exercise was 47 fold greater than resting, and is therefore far beyond this 'collapse threshold'. For this reason, in the absence of ESA, system collapse is observed in the simulations of the severe intensity exercise conditions. Strong ESA allows moderate changes in muscle metabolite concentrations and pH to take place, while $\dot{V}O_2$ can reach values far above this threshold (see Fig. 3B in Liguzinski & Korzeniewski, 2006).

Our comparison of computer simulations with experimental data predicts that a slow decay of ESA during muscle recovery after exercise takes place. The simulated time course of [PCr] during recovery can be fitted to experimental data only when a slow decay of ESA is assumed – otherwise the PCr recovery would be much slower (see Korzeniewski & Zoladz, 2014). The adjusted values of the characteristic ESA decay time $\tau(OFF_{OX})$ were 90 s and 180

s for moderate and severe exercise, respectively. This is consistent with previous suggestions that a greater muscle metabolic strain during exercise lengthens $\tau(OFF_{OX})$, sometimes leading to a transient overshoot in PCr recovery (Korzeniewski & Zoladz, 2005). It seems logical that more intensive exercise causes greater muscle metabolic stress and strain. Therefore, in our simulations ESA was necessary not only to account for the increase in muscle $\dot{V}O_2$ and vOX, and changes in metabolites during the on-transient, but also to explain system behaviour during the off-transient.

The molecular mechanism of ESA remains in question. Glancy et al. (2013) showed that the activity of essentially all OXPHOS complexes was sensitive to Ca^{2+}: isolated skeletal muscle mitochondria incubated with glutamate/malate and exposed to increased Ca^{2+}, increased overall OXPHOS activity by about 2 fold. In electrically-stimulated canine muscle direct measurement of the $\dot{V}O_2$-[ADP] relationship suggested an A_{OX} of ~3-4 fold with a $\tau(ON_{OX})$ of ~10 s (Wüst et al. 2011). The present study strongly suggests that OXPHOS complexes are activated directly over 5 fold during rest-to-work transitions in humans. In other muscles or experimental conditions this direct activation of OXPHOS can be even higher (Korzeniewski, 2014). It was proposed previously that cytosolic Ca^{2+} acts *in vivo* through some protein analogous to calmodulin that causes protein (e.g., OXPHOS complexes) phosphorylation and that is absent in the isolated mitochondrial system (Korzeniewski, 1998; Korzeniewski, 2007; Korzeniewski, 2014).

Generally, the consequence of ESA is that the regulation of OXPHOS in intact skeletal muscle is completely different than in isolated mitochondria (at least in the absence of Ca^{2+}). In other words, the resting state in muscles is different from state 4 in isolated mitochondria: there is some ATP usage for 'basal' ATP usage by reactions that keep the cell alive (RNA/protein synthesis, ion circulation) that is responsible for about 40% of muscle $\dot{V}O_2$ in rat skeletal muscle, with the remaining $\dot{V}O_2$ due to proton leak (Rolfe & Brand, 1996). Additionally, moderate and severe exercise states in intact muscle are different from state 3 in isolated mitochondria: $\dot{V}O_2$, Δp (protonmotive force) and NADH are much greater, while

449 [ADP] and [P_i] are much less in intact muscle (Korzeniewski, 2015). Therefore, experimental
450 data from isolated mitochondria (at least in the absence of Ca^{2+}) concerning the regulation of
451 OXPHOS during increase in energy (ATP) demand cannot be simply extrapolated to intact
452 skeletal muscle.

453 During rest-to-work transitions in skeletal muscle, some moderate increase in [ADP]
454 and [P_i] takes place and therefore the negative-feedback activation by these metabolites co-
455 operates with ESA in the regulation of OXPHOS (the mixed mechanism; Korzeniewski,
456 2014). During work transitions in intact heart *in vivo* metabolite (PCr, P_i, ADP, ATP, NADH)
457 concentrations are essentially constant (see e.g. Katz et al., 1989); in the nomenclature used
458 here, this reflects a 'pure' ESA-controlled system. This is related to the fact that ATP supply
459 is directly activated during low-to-high work transition to the same extent as ATP usage
460 (discussed in detail previously; Korzeniewski et al., 2005; Korzeniewski, 2006; Korzeniewski,
461 2007).

462 While the each-step activation (ESA) mechanism was proposed previously, this study
463 constitutes a very significant advance. Previous studies mostly used a semi-quantitative
464 indirect validation of ESA in relation to steady-state changes in $\dot{V}O_2$ and [ADP] or [PCr]
465 during rest-to-work transitions. This study, however, offers a strictly quantitative direct
466 validation, using: 1. Several different variables ($\dot{V}O_2$, PCr, pH, vOX, vCK, vGL); 2. Whole
467 time courses during rest-work-recovery transitions; 3. Both moderate and severe intensity
468 exercise. The excellent agreement of computer simulations with experimental data for such a
469 broad range of system properties greatly supports the ESA mechanism and increases the
470 computer model reliability.

471 It is in principle possible that a mechanism other than ESA could account for the
472 discussed experimental data. On the other hand, we do not know any likely candidate for
473 such a mechanism. Alternative proposals would have to also explain the great number of
474 different system properties, time and intensity dependence, as explained by the ESA model
475 with strong inhibition of glycolysis by protons, and it seems unlikely that two completely
476 different mechanisms would be able to achieve this. We mean not only the system properties

simulated in the present study, but also numerous other properties, for instance the uniform distribution of metabolic control among OXPHOS complexes or PCr recovery overshoot, discussed previously (Korzeniewski, 2007; Korzeniewski ,2011; Korzeniewski 2014).

Recently Wilson (Wilson, 2015) presented a modified dynamic version of his previous static model (Wilson et al., 1979), involving e.g., the CK system. It was successful in reproducing semi-quantitatively some system properties, for instance the time course of PCr after the onset of exercise. Although the kinetic description of cytochrome oxidase in this model is very complex, the suggestion that cytochrome oxidase determines the rate of oxygen consumption is not well supported by Metabolic Control Analysis of isolated skeletal muscle mitochondria showing that flux control is more or less evenly distributed among OXPHOS complexes (Rossignol et al., 1999). While this model proposes to explain the 'lag phase' in pulmonary or muscle $\dot{V}O_2$ observed in several studies, it remains uncertain the extent to which this lag reflects the mitochondria-lung or mitochondria-muscle vein delay in oxygen transport, rather than an actual lag in mitochondrial $\dot{V}O_2$ on-kinetics. Interpretation of thermodynamic models is complicated because they do not distinguish differing effects of different metabolites e.g. the ADP and P_i. Therefore, in computer modelling it is crucial to validate a model for the broadest set of variable values and system properties possible, we have done here and previously (Korzeniewski, 2007; Korzeniewski ,2011; Korzeniewski 2014; present study).

Mechanisms of the $\dot{V}O_2$ slow component in severe intensity exercise

Our original model of the skeletal muscle bioenergetic system with ATP and H^+ production by anaerobic glycolysis (Korzeniewski & Liguzinski, 2004) included a simple kinetic description of glycolytic inhibition by protons. This description consists of an inverse linear dependence of the glycolytic flux on $[H^+]$ (Equ. 4) and was used in Simulation 1 (Fig. 1). However, Simulation 2 demonstrated that the time course of pH during on-transient measured by Cannon et al. (2014) was much better reproduced when a stronger glycolytic inhibition by $[H^+]$ is assumed (Simulation 2, Fig. 2): specifically an inverse dependence of the

505 glycolytic flux on the cube of proton concentration (Equ. 5) (as well as a much stronger direct
506 glycolysis activation after the onset of exercise). This assumption also worked well for
507 moderate exercise (Simulation 3, Fig. 3). Therefore, this study provides an improved
508 understanding of the kinetics of control and regulation of glycolytic flux by protons.
509 It should be stressed that the kinetic description of the glycolytic inhibition by H^+ in the
510 model is only phenomenological, and may involve many variables, including buffers whose
511 relative contribution to glycolytic inhibition is intensity and/or pH dependent over the
512 physiologic ranges investigated, such as ammonia or inorganic phosphate. The
513 phenomenological proton buffering capacity is taken into account within the model. We found
514 that the current phenomenological model of strong glycolytic inhibition explained well both
515 moderate and severe intensity exercise system kinetics.
516 Korzeniewski & Zoladz (2015) proposed that the two main mechanisms underlying
517 the $\dot{V}O_2$ slow component in skeletal muscle (Poole et al. 1994), at least during cycling
518 exercise, are the gradual inhibition of ATP supply by anaerobic glycolysis by protons
519 accumulating during exercise (together with a slow decay of ATP supply by CK) and a
520 progressive increase in ATP utilization during constant power exercise. While the latter has
521 been frequently supported by experimental studies (for review see e.g., Rossiter et al. 2002;
522 Rossiter, 2011; Poole & Jones, 2012; Cannon et al. 2014), the former proposition specifically
523 linking progressive inhibition of glycolysis to the $\dot{V}O_2$ slow component magnitude
524 (Korzeniewski & Zoladz, 2015) is untested outside of computer simulations.
525 Here we found that the magnitude of the muscle $\dot{V}O_2$ slow component in Simulations
526 1 and 2 was similar to the magnitude of the pulmonary $\dot{V}O_2$ slow component measured by
527 Cannon et al. (2014) for bilateral KE exercise in humans. Specifically, the relative increase in
528 muscle $\dot{V}O_2$ (and vOX) between 3rd and 8th min of exercise was 20 % in both simulations,
529 and the relative increase in pulmonary $\dot{V}O_2$ was 22 % in the measured data. This suggests
530 that either moderate or strong glycolytic inhibition by protons likely contributes to the
531 dynamics of *in vivo* muscle energetics in general, and to the dynamics of the $\dot{V}O_2$ slow
532 component in particular (with strong glycolytic inhibition better reproducing the dynamics of

pH), by necessitating a greater vOX as vGL becomes increasingly inhibited by proton accumulation in severe-intensity exercise in humans.

It has been proposed, on the basis of the lack of correlation between the magnitude of the pulmonary $\dot{V}O_2$ slow component and the 'slow component' of the oxidative ATP supply (vOX), that a decrease in the P/O ratio may contribute to the muscle $\dot{V}O_2$ on-kinetics (Cannon et al. 2014). However, the interpretation of this finding is equivocal.

First, as discussed above, because the average relative increase in pulmonary $\dot{V}O_2$ and in vOX between 3rd and 8th min of exercise are very similar, varying P/O ratio among subjects would imply that in some subjects P/O decreases in the course of exercise, while in other subjects it increases. The latter seems unlikely. An alternative explanation could be a relatively large variability of vOX values (see error bars in Figs. 1-3) measured using the method based on the PCr recovery kinetics.

Second, as discussed in Cannon et al. (2014), there exist complexities associated with inferring muscle $\dot{V}O_2$ kinetics from pulmonary $\dot{V}O_2$ measurements. In this study the experimental pulmonary $\dot{V}O_2$ (including whole-body O_2 uptake) is, naturally, much greater than the simulated muscle $\dot{V}O_2$ (isolated to the active muscle *in silico*) estimated from the oxidative ATP supply (vOX). Using pulmonary gas exchange measurements to infer kinetic changes across the skeletal muscle requires a number of assumptions, including that the metabolic contribution of 'resting tissues' (basal metabolism in all bodily tissues) and 'auxiliary tissues' (activity of respiratory muscles, stabilizing muscles, cardiac muscle etc.) are constant during constant power exercise. With cycling exercise or seated single leg KE exercise, this assumption appears reasonable (e.g. Grassi et al., 1996; Krustrup et al., 2009), and thus the $\dot{V}O_2$ slow component can be inferred to be predominantly isolated to the active locomotor muscles (Poole et al. 1991). The study of Cannon et al. (2014) used bilateral KE exercise inside a superconducting magnet to measure phosphate metabolism by ^{31}P MRS while maximizing the muscle mass engaged in the task and simulate conditions such as in walking or cycling. In this model, the contribution of 'axillary tissues' appears to be as much as approximately 35 to 45 % of the pulmonary $\dot{V}O_2$ (assuming 6 or 5 kg of the mass of two

561 active quadriceps, respectively). Importantly it is not known whether oxygen consumption by
562 these tissues changes substantially during exercise; any increase would contribute to the
563 magnitude of the pulmonary $\dot{V}O_2$ slow component, but not vOX or $\dot{V}O_2$ in the muscles of
564 interest.

565 During severe cycling exercise, working muscles are responsible for about 85 % of
566 pulmonary $\dot{V}O_2$ (Poole et al. 1992), while ATP supply by 'auxiliary tissues' is about 8 % (as
567 estimated by Liguzinski & Korzeniewski, 2007), with the remainder being due to metabolism
568 in 'resting tissues'. It seems that this relative contribution is much smaller in severe KE
569 exercise, where the muscle mass activated for the external KE power production is smaller
570 than in running or cycling. Additionally, the only known process that could decrease P/O,
571 namely proton leak through the inner mitochondrial membrane, is estimated to be
572 responsible for only about 1 % of muscle $\dot{V}O_2$ during severe exercise (Korzeniewski &
573 Zoladz, 2015), reducing the likelihood that mitochondrial uncoupling contributes substantially
574 to the muscle $\dot{V}O_2$ slow component magnitude. Finally, a significant (about 20 % at rest)
575 fraction of O_2 is consumed in the skeletal muscle cell by non-mitochondrial processes
576 (residual oxygen consumption by e.g. NAPDH oxidase, nitric oxide synthase, or xanthine
577 oxidase), and not by OXPHOS in mitochondria (Rolfe et al. 1999). However, it cannot be
578 excluded currently that a decrease in P/O contributes to some extent to the muscle $\dot{V}O_2$ slow
579 component on transition to KE exercise.

580 We did not model the experimentally-measured pulmonary $\dot{V}O_2$ (Cannon et al. 2014),
581 because, as discussed above, the ratio of 'active' to 'axillary' and 'resting' tissues $\dot{V}O_2$ is
582 unknown and may vary during exercise, and the outcome of the simulation rests entirely on
583 the ratio selected. Additionally, it is likely that a slow decay of $\dot{V}O_2$ by 'auxiliary tissues' and
584 the contribution of circulatory dynamics to O_2 transport may dissociate pulmonary $\dot{V}O_2$
585 kinetics from the muscle (Barstow et al., 1990; Benson et al. 2013; Korzeniewski & Zoladz,
586 2013), especially during recovery (Krustrup et al. 2009). Instead, for comparison with
587 simulated data, we relied on the on-transition vOX measured from ^{31}P MRS in Cannon et al.

588 (2014), but we have no independent estimation of vOX in recovery other than that inferred
589 from [PCr] recovery kinetics.
590
591 *Data variability*
592 We adjusted our model by parameter fitting to averaged data presented in Cannon et
593 al. (2014). However, there is, naturally, some variability in the original data, which may derive
594 either from real differences between individuals ("individual variability") or from variability
595 inherent in the measurement methods ("method variability"). The variability of most variables
596 in Cannon et al. (2014) is moderate, reflecting mostly "individual variability". The only
597 exception is vOX, which was especially variable during moderate intensity exercise. vOX is
598 determined from the initial rate of change of PCr recovery kinetics, and therefore is
599 influenced by the magnitude of the exercise-induced PCr depletion (Rossiter et al., 2000). In
600 this case, the "method variability" is likely the major contributor to the overall variability in
601 moderate intensity vOX, and is within the variability expected for this method (Rossiter et al.,
602 2000).
603 We investigated the potential role of "individual variability", using slight modifications
604 of relevant parameter values in the computational model, for instance A_{OX}, A_{GL}, A_{UT} and/or
605 OXPHOS activity (there is no reason for these values to be identical among different
606 individuals). The "individual variability" can be due to e.g. genetic differences or physical
607 training. It has been proposed that training may lead not only to an increase in OXPHOS
608 activity related to mitochondrial biogenesis, but also to elevation of ESA intensity (increase of
609 A_{OX}) (Korzeniewski & Zoladz, 2003; Korzeniewski & Zoladz, 2004). It was demonstrated that
610 both effects lead to acceleration of the $\dot{V}O_2$ on-kinetics and to improvement of metabolite
611 stability during rest-to-work transitions (Korzeniewski & Zoladz, 2003; Korzeniewski &
612 Zoladz, 2004). Overall, we found that small modifications of relevant parameter values in the
613 computational model could well account for the "individual variability" observed in several
614 parameter values in moderate and severe intensity exercise. We also believe that the
615 apparent (although not statistically significant) overshoot in vOX in moderate exercise is

predominately due to “method variability”; however a direct identification of the source of this variability remains to be determined.

Conclusions

The computer model of the skeletal muscle cell bioenergetic system developed previously (Korzeniewski, 1998; Korzeniewski & Zoladz, 2001; Korzeniewski & Liguzinski, 2004) reproduces very well the experimental data of the time courses of [PCr] and pH during rest-work-rest transitions, as well as the ATP synthesis rate by OXPHOS (vOX), creatine kinase (vCK) and anaerobic glycolysis (vGL) after 3 and 8 min of moderate and severe bilateral knee extension (KE) exercise in humans (Cannon et al. 2014). It is demonstrated that an intensive each-step-activation (ESA) (over 5-fold direct activation of all OXPHOS complexes and NADH supply in parallel with the activation of ATP usage) was necessary to account for the changes in ATP synthesis fluxes, PCr and pH encountered in human muscles *in vivo*. Also a slow decay of ESA during recovery was necessary to fit experimental data. A strong inhibition of glycolysis by protons improves the agreement between the simulated and measured kinetics of pH after the onset of exercise in comparison to a moderate glycolytic inhibition. It is postulated that strong inhibition by accumulating protons of ATP supply by anaerobic glycolysis (together with a slow decay of ATP supply by CK) and an ‘additional’ ATP usage increasing gradually during severe exercise can explain the relative magnitude of the muscle $\dot{V}O_2$ slow component, although some contribution of a decrease in P/O cannot be explicitly excluded. Overall, this well-tested computer model provides a useful tool for studying the dynamic behaviour of muscle metabolism during exercise and recovery.

ADDITIONAL INFORMATION

Competing interests

None.

Acknowledgements

The authors thank Dr. Daniel Cannon for his collaboration in providing the original data for comparison with the simulations made in this study.

Author contribution

B.K. and H.B.R. designed computer simulations. H.B.R. prepared experimental data for presentation. B.K. performed computer simulations and prepared figures. B.K. and H.B.R. discussed the theoretical results and wrote the manuscript. Both authors critically reviewed and approved the final version of the manuscript.

Funding

The experimental data collection was supported by Biotechnology and Biological Sciences Research Council (BBSRC) UK BB/I001174/1 and BB/I00162X/1.

REFERENCES

Barstow TJ & Mole PA (1991). Linear and nonlinear characteristics of oxygen uptake kinetics during heavy exercise. *J Appl Physiol* **71**, 2099-2106.

Barstow TJ, Lamarra N & Whipp BJ (1990). Modulation of muscle and pulmonary O_2 uptakes by circulatory dynamics during exercise. *J Appl Physiol* **68**, 979-989.

Benson AP, Grassi B & Rossiter HB (2013). A validated model of oxygen uptake and circulatory dynamic interactions at exercise onset in humans. *J Appl Physiol* **115**, 743-755.

Chance B & Williams GR (1955). Respiratory enzymes in oxidative phosphorylation. I. Kinetics of oxygen utilization. *J Biol Chem* **217**, 383-393.

Cannon DT, Bimson WE, Hampson SA, Bowen TS, Murgatroyd SR, Marwood S, Kemp GJ & Rossiter HB (2014). Skeletal muscle ATP turnover by ^{31}P magnetic resonance spectroscopy during moderate and heavy bilateral knee extension. *J Physiol* **592**, 5287-5300.

Connet R & Sahlin K (1996). Control of glycolysis and glycogen metabolism. In *Handbook of physiology*, ed. Rowell L & Shepherd J, pp. 870-911. New York, Oxford University Press.

Denton RM & McCormack JG (1990). Ca^{2+} as a second messenger within mitochondria of the heart and other tissues. *Annu Rev Physiol* **52**, 451–466.

Gellerich F N, Gizatullina Z, Trumbekaite S, Korzeniewski B, Gaynutdinov T, Seppet E, Vielhaber S & Heinze H-J, Striggow F (2012). Cytosolic Ca^{2+} regulates the energization of isolated brain mitochondria by formation of pyruvate through the malate-aspartate shuttle. *Biochem J* **443**, 747–755.

Glancy B, Willis WT, Chess DJ & Balaban RS (2013). Effect of calcium on the oxidative phosphorylation cascade in skeletal muscle mitochondria. *Biochemistry* **52**, 2793-2809.

Grassi B, Poole DC, Richardson RS, Knight DR, Erickson BK & Wagner PD (1996). Muscle O_2 uptake kinetics in humans: implications for metabolic control. *J Appl Physiol* **80**, 988-998.

684 Hansford RG (1980). Control of mitochondrial substrate oxidation. *Curr Top Bioenerg* **10**,
685 217-277.
686 Hochachka P (1994). *Muscles as metabolic machines*. CRC Press, Boca Raton.
687 Jeneson JA, Wiseman RW, Westerhoff HV & Kushmerick MJ (1996). The signal transduction
688 function of oxidative phosphorylation is at least second order in ADP. *J Biol Chem* **271**,
689 27995-27998.
690 Jones AM, Wilkerson DP, DiMenna F, Fulford J, Poole DC (2008). Muscle metabolic
691 responses to exercise above and below the "critical power" assessed using 31P-MRS. *Am*
692 *J Physiol Regul Integr Comp Physiol* **294**, R585-R593.
693 Katz LA, Swain JA, Portman MA & Balaban RS (1989). Relation between phosphate
694 metabolites and oxygen consumption of heart in vivo. *Am J Physiol* **256**, H265-H274.
695 Korzeniewski B (1998). Regulation of ATP supply during muscle contraction: theoretical
696 studies. *Biochem J* **330**, 1189-1195.
697 Korzeniewski B (2003). Regulation of oxidative phosphorylation in different muscles and
698 various experimental conditions. *Biochem J* **375**, 799-804.
699 Korzeniewski B (2006). Oxygen consumption and metabolite concentrations during
700 transitions between different work intensities in heart. *Am J Physiol* **291**, 1466-1471.
701 Korzeniewski B (2007). Regulation of oxidative phosphorylation through parallel activation.
702 *Biophys Chem* **129**, 93-110.
703 Korzeniewski B (2011). Computer-aided studies on the regulation of oxidative
704 phosphorylation during work transitions. *Prog Biophys Mol Biol* **107**, 274-285.
705 Korzeniewski B (2014). Regulation of oxidative phosphorylation during work transitions
706 results from its kinetic properties. *J Appl Physiol* **116**, 83-94.
707 Korzeniewski B (2015). 'Idealized' state 4 and state 3 in mitochondria vs. rest and work in
708 skeletal muscle. *PLoS One* **10** (2): e0117145. doi: 10.1371/journal.pone.0117145.
709 Korzeniewski B & Liguzinski P (2004). Theoretical studies on the regulation of anaerobic
710 glycolysis and its influence on oxidative phosphorylation in skeletal muscle. *Biophys*
711 *Chem* **110**, 147-169.

712 Korzeniewski B, Noma A & Matsuoka S (2005). Regulation of oxidative phosphorylation in
713 intact mammalian heart in vivo. *Biophys Chem* **116**, 145-157.
714 Korzeniewski B & Zoladz JA (2001). A model of oxidative phosphorylation in mammalian
715 skeletal muscle. *Biophys Chem* **92**, 17-34.
716 Korzeniewski B & Zoladz JA (2003). Training-induced adaptation of oxidative
717 phosphorylation in skeletal muscle. *Biochem J* **374**, 37-40.
718 Korzeniewski B & Zoladz JA (2004). Factors determining the oxygen consumption rate ($\dot{V}O_2$)
719 on-kinetics in skeletal muscle. *Biochem J* **375**, 799-804.
720 Korzeniewski B & Zoladz JA (2005). Some factors determining the PCr recovery overshoot in
721 skeletal muscle. *Biophys Chem* **116**, 129-136.
722 Korzeniewski B & Zoladz JA (2013). Slow $\dot{V}O_2$ off-kinetics in skeletal muscle is associated
723 with fast PCr off-kinetics – and inversely. *J Appl Physiol* **115**, 605-612.
724 Korzeniewski B & Zoladz JA (2015). Possible mechanisms underlying slow component of
725 $\dot{V}O_2$ on-kinetics in skeletal muscle. *J Appl Physiol* **118**, 1240-1249.
726 Krustrup P, Jones AM, Wilkerson DP, Calbet JA & Bangsbo J (2009). Muscular and
727 pulmonary O_2 uptake kinetics during moderate- and high-intensity sub-maximal knee-
728 extensor exercise in humans. *J Physiol* **587**, 1843–1856.
729 Kushmerick MJ (1997). Multiple equilibria of cations with metabolites in muscle
730 bioenergetics. *Am J Physiol* **272**, C1739-C1747.
731 Liguzinski P & Korzeniewski B (2006). Metabolic control over the oxygen consumption flux in
732 intact skeletal muscle: in silico studies. *Am J Physiol* **291**, C1213-C1224.
733 Liguzinski P & Korzeniewski B (2007). Oxygen delivery by blood determines the maximal
734 $\dot{V}O_2$ and work rate during whole body exercise in humans: in silico studies. *Am J Physiol*
735 **293**, H343-H353.
736 McCormack JG (1990). Ca^{2+} as a second messenger within mitochondria of the heart and
737 other tissues. *Annu Rev Physiol* **52**, 451–466.
738 Paterson & Whipp (1991). Asymmetries of oxygen uptake transients at the on- and offset of
739 heavy exercise in humans. *J Physiol* **443**, 575-86.

740 Poole DC, Barstow DJ, Gaesser GA, Willis WT & Whipp BJ (1994). $\dot{V}O_2$ slow component:
741 physiological and functional significance. *Med Sci Sports Exerc* **26**, 1354-1358.
742 Poole DC, Gaesser GA, Hogan MC, Knight DR & Wagner PD (1992). Pulmonary and leg
743 $\dot{V}O_2$ during submaximal exercise: implications for muscular efficiency. *J Appl Physiol* **72**,
744 805-810.
745 Poole DC & Jones AM (2012). Oxygen uptake kinetics. *Compr Physiol* **2**, 933-996.
746 Poole DC, Schaffartzik W, Knight DR, Derion T, Kennedy B, Guy HJ, Prediletto R & Wagner
747 PD (1991). Contribution of exercising legs to the slow component of oxygen uptake
748 kinetics in humans. *J Appl Physiol* **71**, 1245–1253.
749 Poole DC, Ward SA, Gardner GW, Whipp BJ (1988). Metabolic and respiratory profile of the
750 upper limit for prolonged exercise in man. *Ergonomics* **31**, 1265-1279.
751 Rolfe DFS & Brand MD (1996). Proton leak and control of oxidative phosphorylation in
752 perfused, resting rat skeletal muscle. *Biochim Biophys Acta* **1276**, 45-50.
753 Rolfe DFS, Newman JMB, Buckingham JA, Clark MG & Brand MD (1999). Contribution of
754 mitochondrial proton leak to respiration rate in working skeletal muscle and liver and to
755 SMR. *Am J Physiol* **276**, C692-699.
756 Rossignol R, Letellier T, Malgat M, Rocher C & Mazat J-P (2000). Tissue variation in the
757 control of oxidative phosphorylation. *Biochem J* **347**, 45-53.
758 Rossiter HB (2011). Exercise: Kinetic considerations for gas exchange. *Compr Physiol* **1**,
759 203-244.
760 Rossiter HB, Howe FA, Ward SA, Kowalchuk JM, Griffiths JR & Whipp BJ (2000).
761 Intersample fluctuations in phosphocreatine concentration determined by 31P-magnetic
762 resonance spectroscopy and parameter estimation of metabolic responses to exercise in
763 humans. *J Physiol* **528**, 359-369.
764 Rossiter HB, Ward SA, Kowalchuk JM, Howe FA, Griffiths JR & Whipp BJ (2002). Dynamic
765 asymmetry of phosphocreatine concentration and O_2 uptake between the on- and off-
766 transients of moderate- and high-intensity exercise in humans. *J Physiol* **541**, 991–1002.

767 Sutton JR, Jones NL & Toews CJ (1981). Effect of pH on muscle glycolysis during exercise.
768 *Clin Sci (Lond)* **61**, 331-338.
769 Wilson DF (2015). Regulation of metabolism: the rest to work transition in skeletal muscle.
770 Am J Physiol Endocrinol Metab, doi: 10.1152/ajpendo.00355.2015.
771 Wilson DF, Owen CS & Erecińska M (1979). Quantitative dependence of mitochondrial
772 oxidative phosphorylation on oxygen concentration: A mathematical model. *Arch Biochem*
773 *Biophys* **195**, 494-504.
774 Wu F, Jeneson JAL & Beard, DA (2007). Oxidative ATP synthesis in skeletal muscle is
775 controlled by substrate feedback. *Am J Physiol Cell Physiol* **292**, C115-C124.
776 Wüst RCI, Grassi B, Hogan MC, Howlett RA, Gladden LB & Rossiter HB (2011). Kinetic
777 control of oxygen consumption during contractions in self-perfused skeletal muscle. *J*
778 *Physiol* **589**, 3995-4009.
779 Zoladz JA, Gladden LB, Hogan MC, Nieckarz Z & Grassi B (2008). Progressive recruitment
780 of muscle fibers is not necessary for the slow component of $V'O_2$ on-kinetics. *J Appl*
781 *Physiol* **105**, 575-580.

FIGURE LEGENDS

Fig. 1. Comparison of simulated (lines) and experimental (points) time course of PCr (% of resting values), pH and ATP supply flux during severe intensity rest-exercise-recovery with moderate glycolytic inhibition by protons (Simulation 1). Time course of simulated muscle $\dot{V}O_2$ and ADP are also presented. Experimental points for bilateral knee extension (KE) exercise in humans were taken from Cannon et al. (2014). Vertical lines in the upper panel indicate the onset and cessation of exercise. vOX, ATP supply rate by OXPHOS; vCK, ATP supply rate by CK; vGL, ATP supply rate by anaerobic glycolysis; vUT, muscle ATP utilization (ATP hydrolysis). 0.05 was subtracted from experimental pH values in order to scale experimental pH at rest to the value of 7.0, used in computer simulations.

Fig. 2. Comparison of simulated (lines) and experimental (points) time course of PCr (% of resting values), pH and ATP supply flux during severe intensity rest-exercise-recovery transitions with strong glycolytic inhibition by protons (Simulation 2). Time course of simulated muscle $\dot{V}O_2$ and ADP are also presented. Experimental points for bilateral knee extension (KE) exercise in humans were taken from Cannon et al. (2014). Vertical lines in the upper panel indicate the onset and cessation of exercise. vOX, ATP supply rate by OXPHOS; vCK, ATP supply rate by CK; vGL, ATP supply rate by anaerobic glycolysis; vUT, muscle ATP utilization (ATP hydrolysis). 0.05 was subtracted from experimental pH values in order to scale experimental pH at rest to the value of 7.0, used in computer simulations.

Fig. 3. Comparison of simulated (lines) and experimental (points) time course of PCr (% of resting values), pH and ATP supply flux during moderate intensity rest-exercise-recovery transitions with strong glycolytic inhibition by protons (Simulation 3). Time course of simulated muscle $\dot{V}O_2$ and ADP are also presented. Experimental points for bilateral knee extension (KE) exercise in humans were taken from Cannon et al. (2014). Vertical lines in the upper panel indicate the onset and cessation of exercise. vOX, ATP supply rate by OXPHOS; vCK, ATP supply rate by CK; vGL, ATP supply rate by anaerobic glycolysis; vUT,

808 muscle ATP utilization (ATP hydrolysis). 0.08 was subtracted from experimental pH values in
809 order to scale experimental pH at rest to the value of 7.0, used in computer simulations.

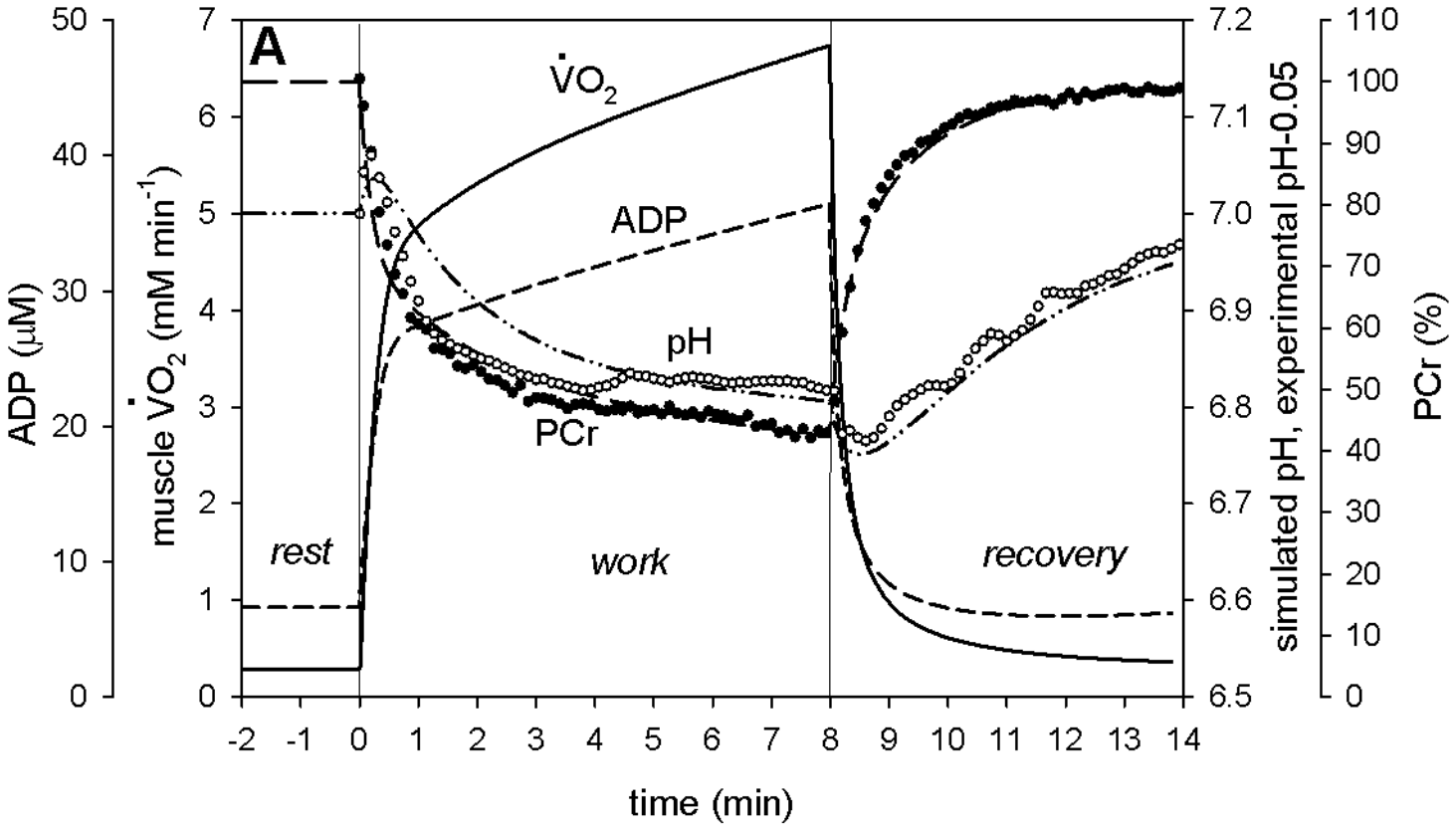
A
$\dot{V}O_2$
ADP
pH
PCr
rest
work
recovery
ADP (μM)
muscle $\dot{V}O_2$ (mM min^{-1})
simulated pH, experimental pH-0.05
PCr (%)
time (min)

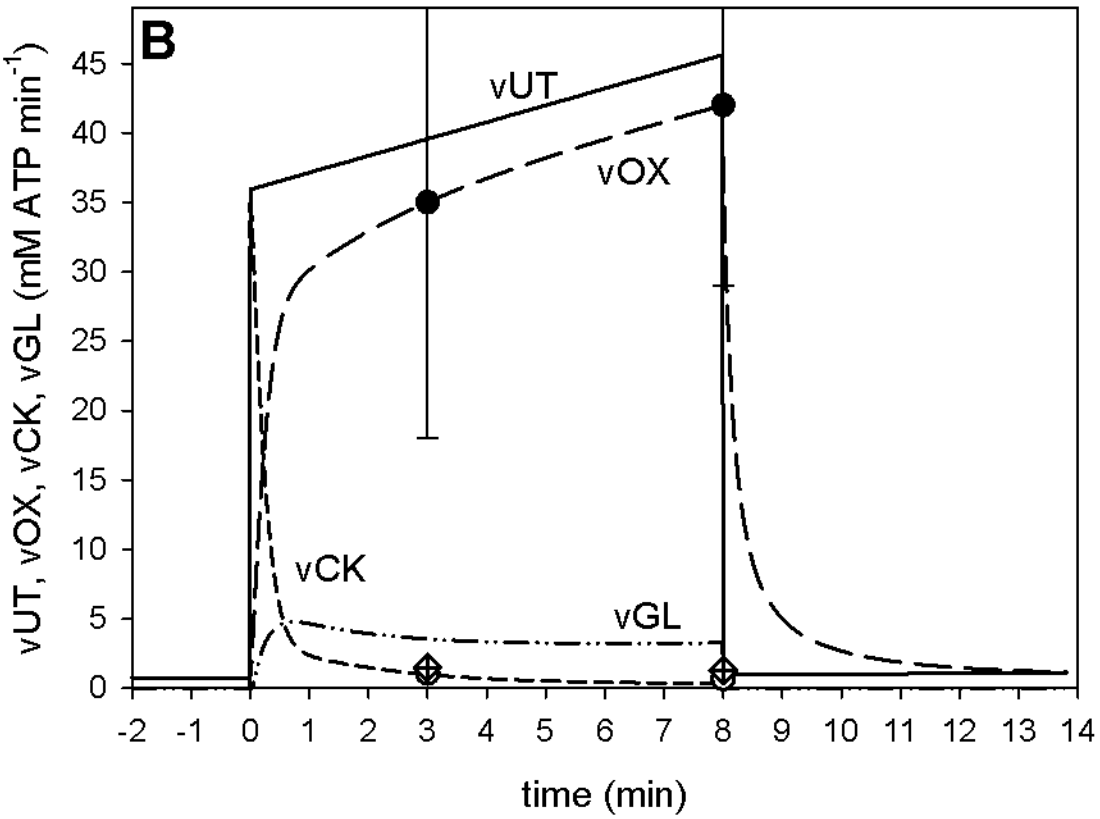
B
vUT
vOX
vCK
vGL
vUT, vOX, vCK, vGL (mM ATP min^{-1})
time (min)

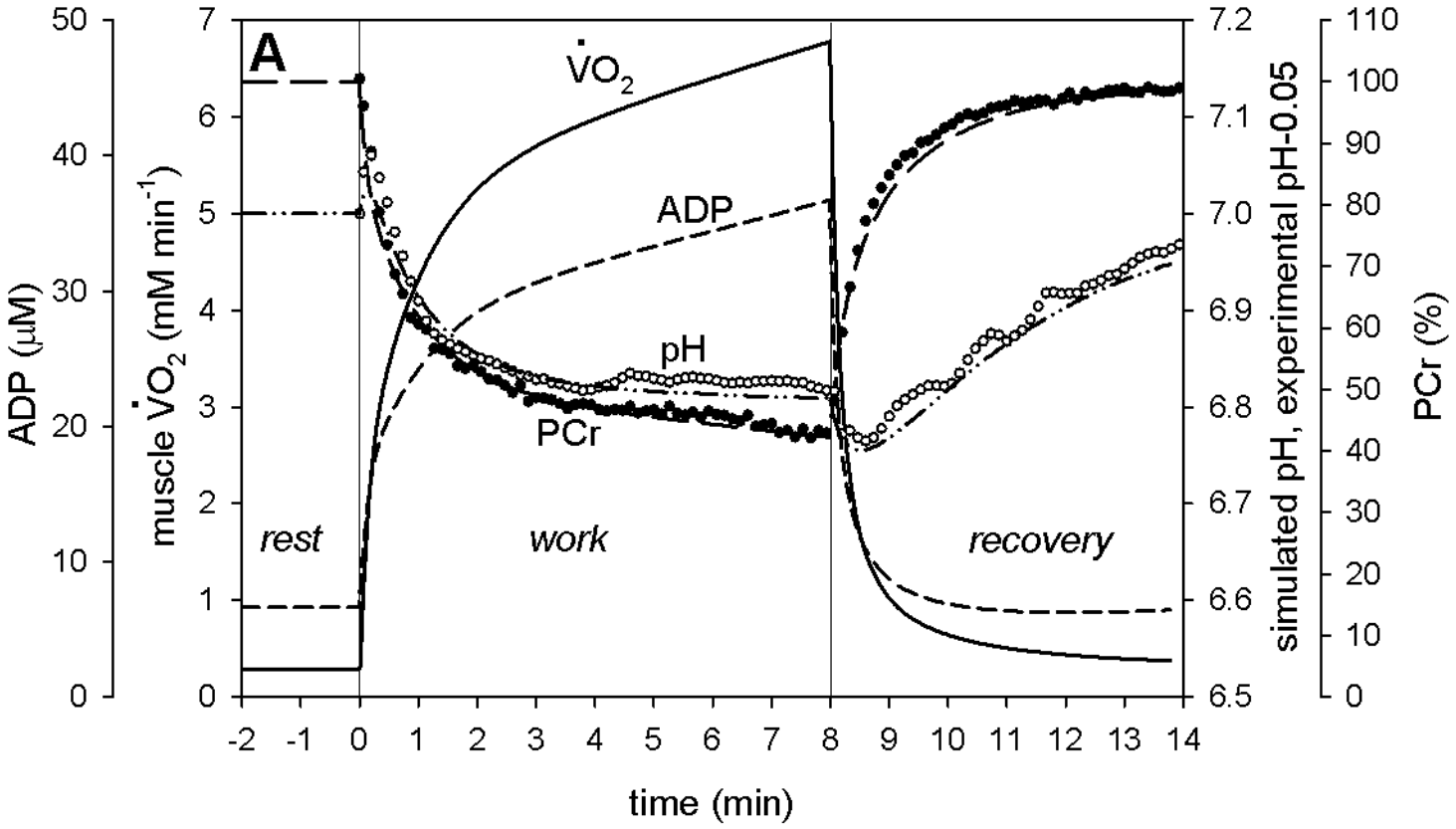
A
$\dot{V}O_2$
ADP
pH
PCr
rest
work
recovery
ADP (μM)
muscle $\dot{V}O_2$ (mM min^{-1})
simulated pH, experimental pH-0.05
PCr (%)
time (min)

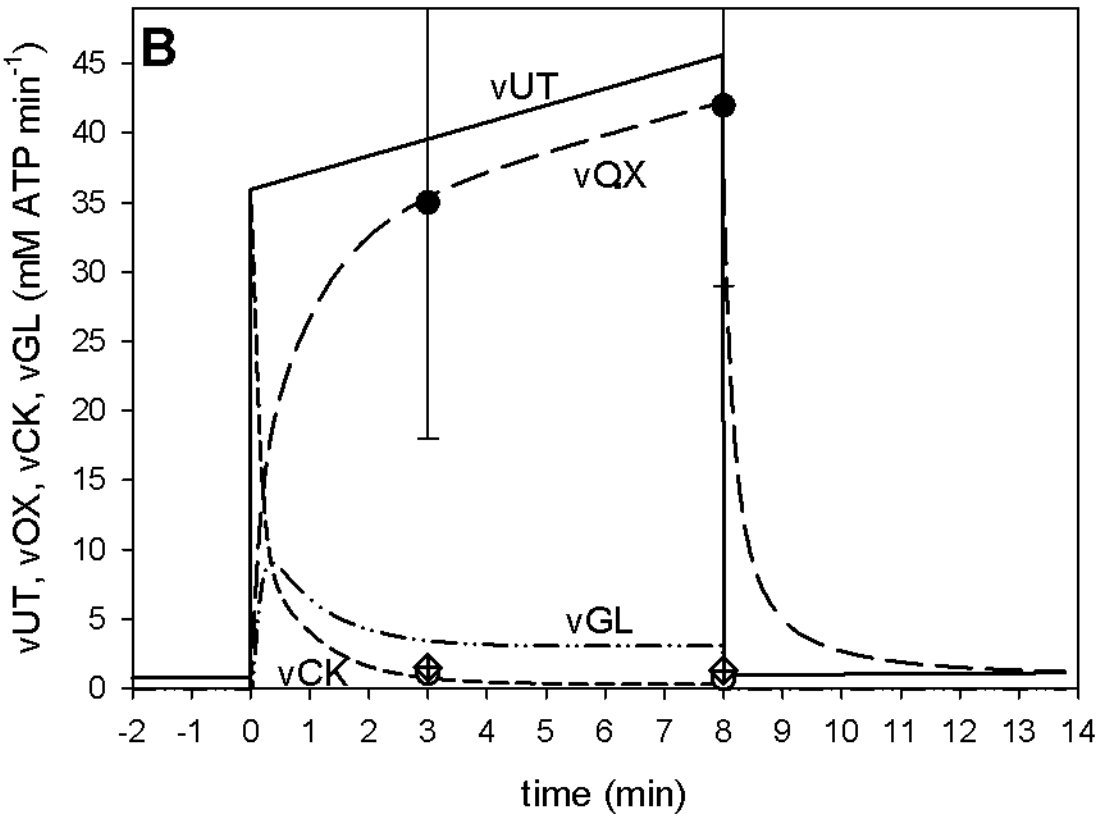
B
vUT
vQX
vGL
vCK
vUT, vOX, vCK, vGL (mM ATP min^{-1})
time (min)

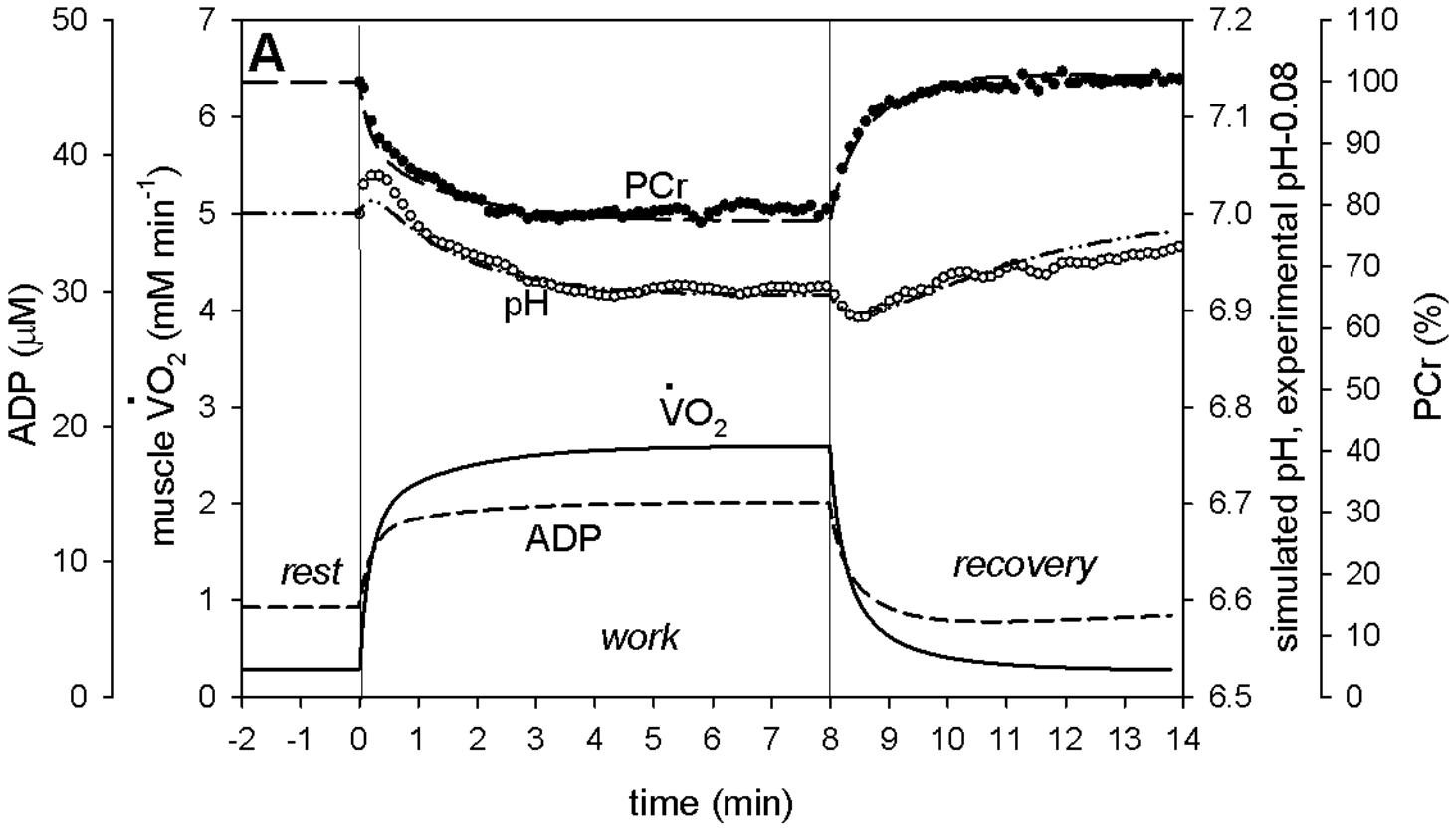
A
ADP (μM)
muscle $\dot{V}O_2$ (mM min^{-1})
simulated pH, experimental pH-0.08
PCr (%)
PCr
pH
$\dot{V}O_2$
ADP
rest
work
recovery
time (min)

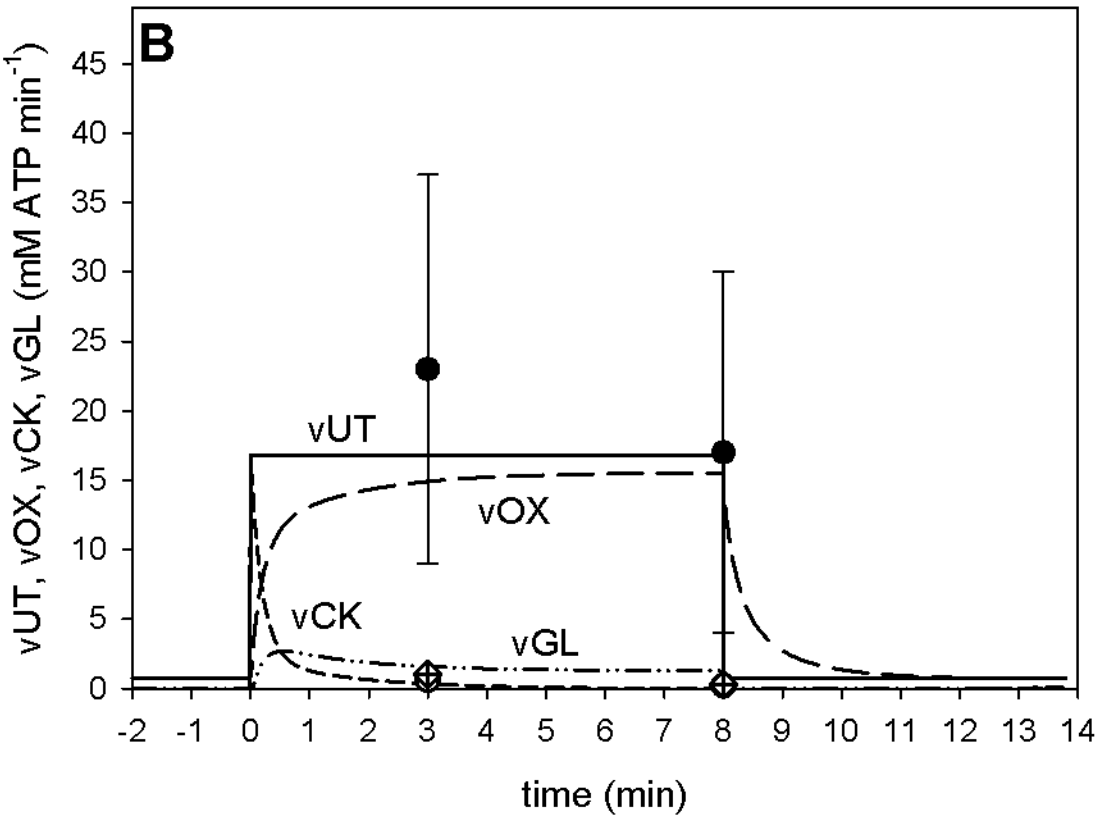
B
vUT, vOX, vCK, vGL (mM ATP min^{-1})
vUT
vOX
vCK
vGL
time (min)